SUPPORTING INFORMATION

Liquid Crystal Emulsions that Intercept and Report on Bacterial Quorum Sensing

Benjamin J. Ortiz,[1,†] Michelle E. Boursier,[2,§] Kelsey L. Barrett,[3] Daniel E. Manson,[2] Daniel Amador-Noguez,[3] Nicholas L. Abbott,[1,‡] Helen E. Blackwell,[2,*] and David M. Lynn[1,2,*]

[1]Dept. of Chemical and Biological Engineering, Univ. of Wisconsin–Madison, 1415 Engineering Dr., Madison, WI 53706; [2]Dept. of Chemistry, Univ. of Wisconsin–Madison, 1101 University Ave., Madison, WI 53706, USA; [3]Dept. of Bacteriology, Univ. of Wisconsin–Madison, 1550 Linden Dr., Madison, WI 53706; [†]Current address: Abbvie, Inc., 1 N. Waukegan Road, North Chicago, IL 60064 [§]Current address: Amgen, Inc., 1 Amgen Center Dr., Thousand Oaks, CA 91320; [‡]Current address: Dept. of Chemical and Biomolecular Engineering, Cornell Univ., Ithaca, NY 14853; Email: (H.E.B.) blackwell@chem.wisc.edu; (D.M.L.) dlynn@engr.wisc.edu

Contents **Page**

Table S1: *P. aeruginosa* strains used in this study S2

Figure S1: Representative scattering plots for LC droplets S3

Figure S2: Percent of LC droplets transformed as function of amphiphile concentration (no fit) S4

Figure S3: Percent of LC droplets transformed as function of amphiphile concentration (with fit) S5

Figure S4: QS pathways used by *P. aeruginosa* to control rhamnolipid synthesis S6

Figure S5: Optical density of bacterial cultures at 0, 6, 12, and 24 h S7

Figure S6: Cell viability upon incubation with LC droplets S7

Quantification of AHL and Rhamnolipid Concentrations in Bacterial Cultures S8

Figure S7: Conc. of AHL and rhamnolipids measured in supernatants S8

Figure S8: Conc. of hydrolyzed and unhydrolyzed AHLs measured in supernatants S12

Figure S9: Conc. of total hydrolyzed and unhydrolyzed AHLs measured in supernatants S13

Supplementary Chemical Methods S14

Scheme 1: Synthesis of racemic 3-(3-hydroxyalkanoyloxy)alkanoic acid S14

NMR spectra for synthetic intermediates 1–6 and HAA S20

References S28

Table S1. *P. aeruginosa* strains used in this study.

Strain	Description*	Reference
PAO1	Wild-type, isolated by B. Holloway from human wound.	[1]
PW6886 (Δ*rhlA*)	PAO1 rhlA-E08::ISphoA/hah, Tc^R	[2]
PAO1 Δ*rhlB*	PAO1 containing an unmarked, in-frame *rhlB* deletion	[3]
PAO-SC4 (Δ*lasI*, Δ*rhlI*)	PAO1 containing unmarked, in-frame *rhlI* and *lasI* deletions	Gift from E. P. Greenberg

* Abbreviations: Tc^R, tetracycline resistance

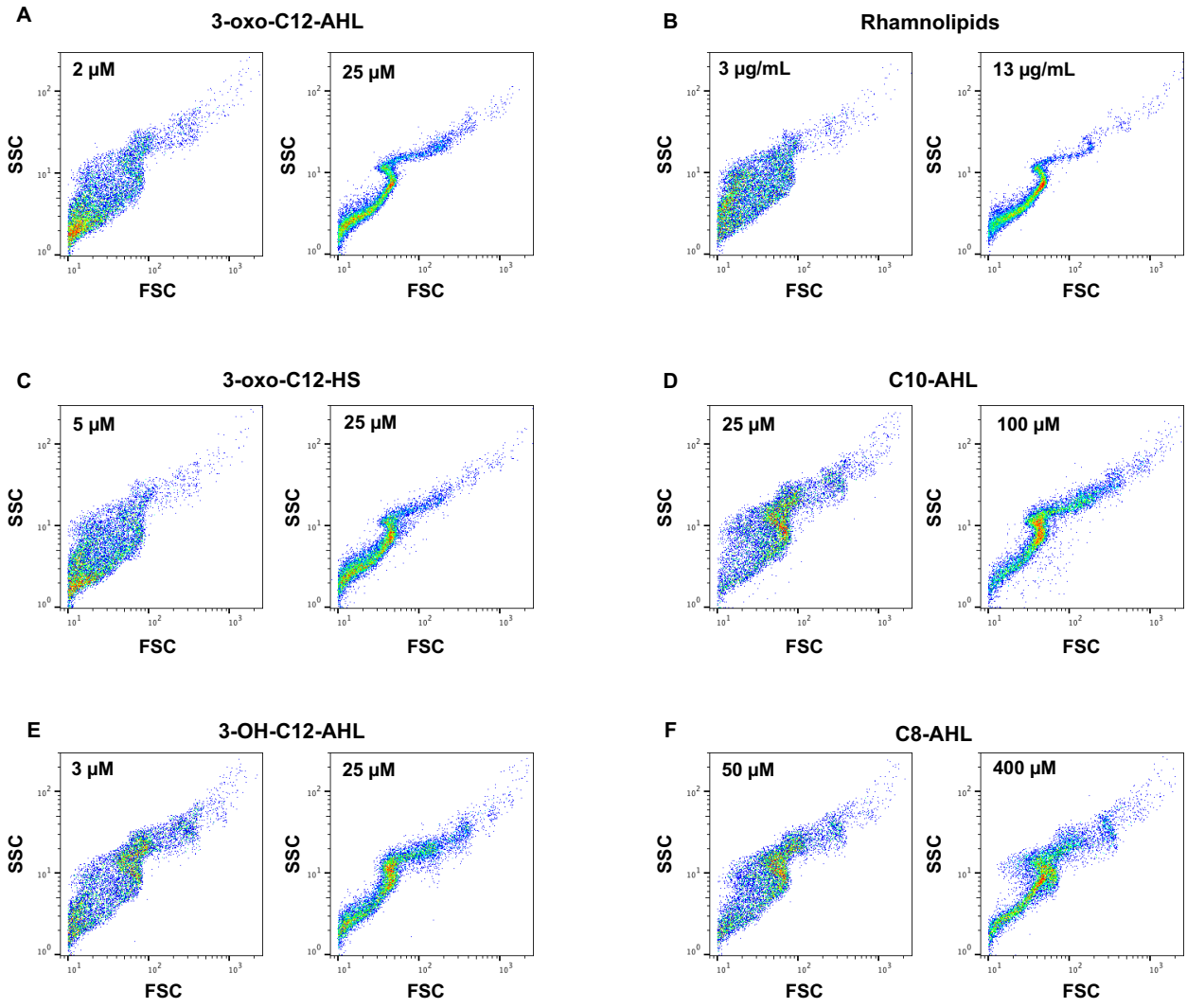

Figure S1. (A-F) Representative SSC vs. FSC plots (scattering plots) for (left) a sample of bipolar LC droplets and (right) a sample of radial droplets arising from exposure to (A) 3-oxo-C12-AHL at a concentration of 2 μM (left) and 25 μM (right), (B) rhamnolipid at a concentration of 3 μg/mL (left) and 13 μg/mL (right), (C) 3-oxo-C12-HS at a concentration of 5 μM (left) and 25 μM (right), (D) C10-AHL at a concentration of 25 μM (left) and 100 μM (right), (E) 3-OH-C12-AHL at a concentration of 3 μM (left) and 25 μM (right), and C8-AHL at a concentration of 50 μM (left) and 400 μM (right). The S-shaped curve observed for the AHL and rhamnolipid-treated droplets is consistent with the results of past reports [see SI references 7 and 8] on the use of flow cytometry to characterize surfactant-treated LC droplets and is characteristic of LC droplet emulsions composed entirely of radial droplets.

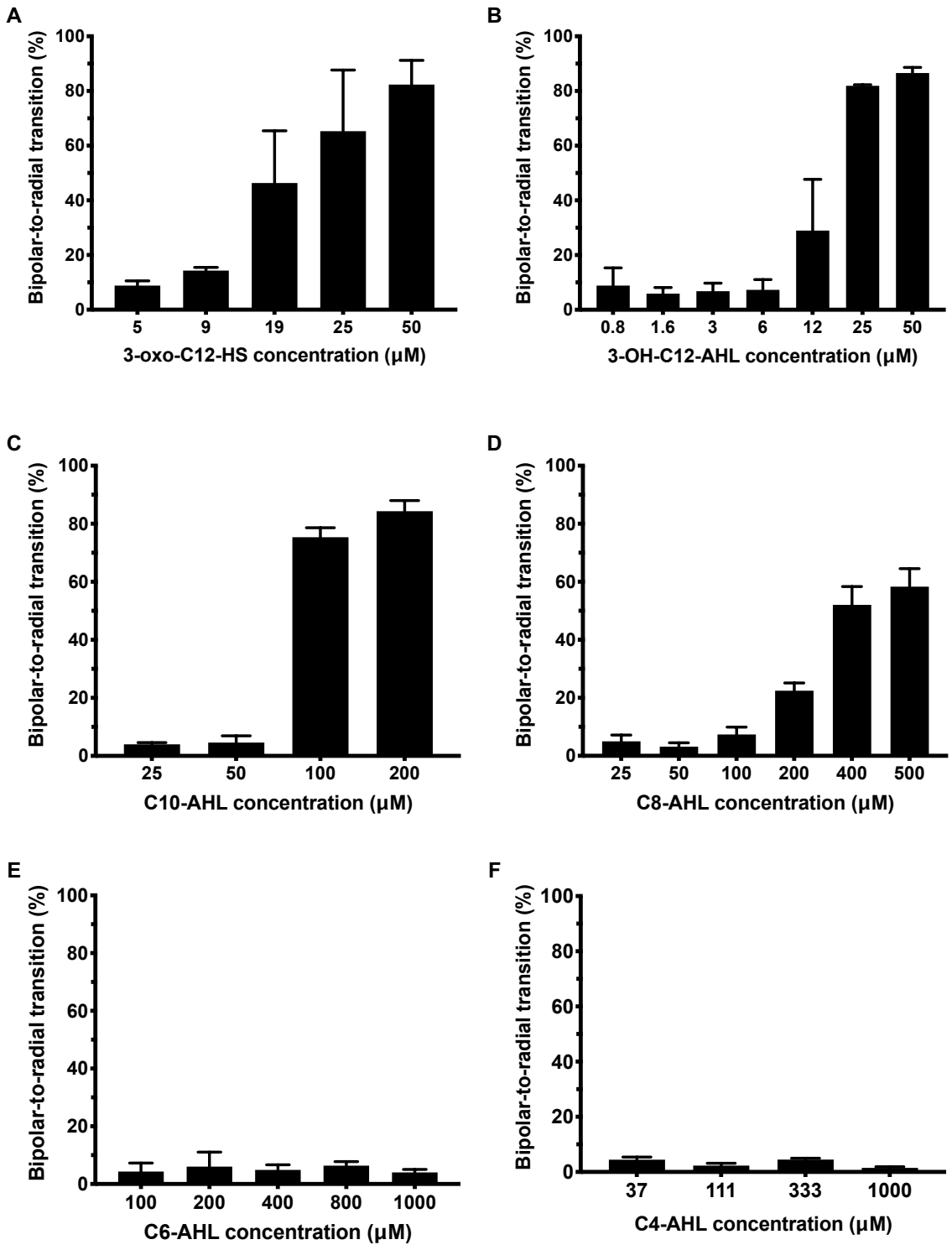

Figure S2. Percentage of droplets transformed from bipolar-to-radial as a function of the concentration of (A) 3-oxo-C12-HS, (B) 3-OH-C12-AHL, (C) C10-AHL, (D) C8-AHL, (E) C6-AHL, (F) C4-AHL in PBS with 10 µM SDS and 1% DMSO. Plots are representative of 3 independent experiments with error bars representing the SEM. Values were obtained from analysis of scattering plots.

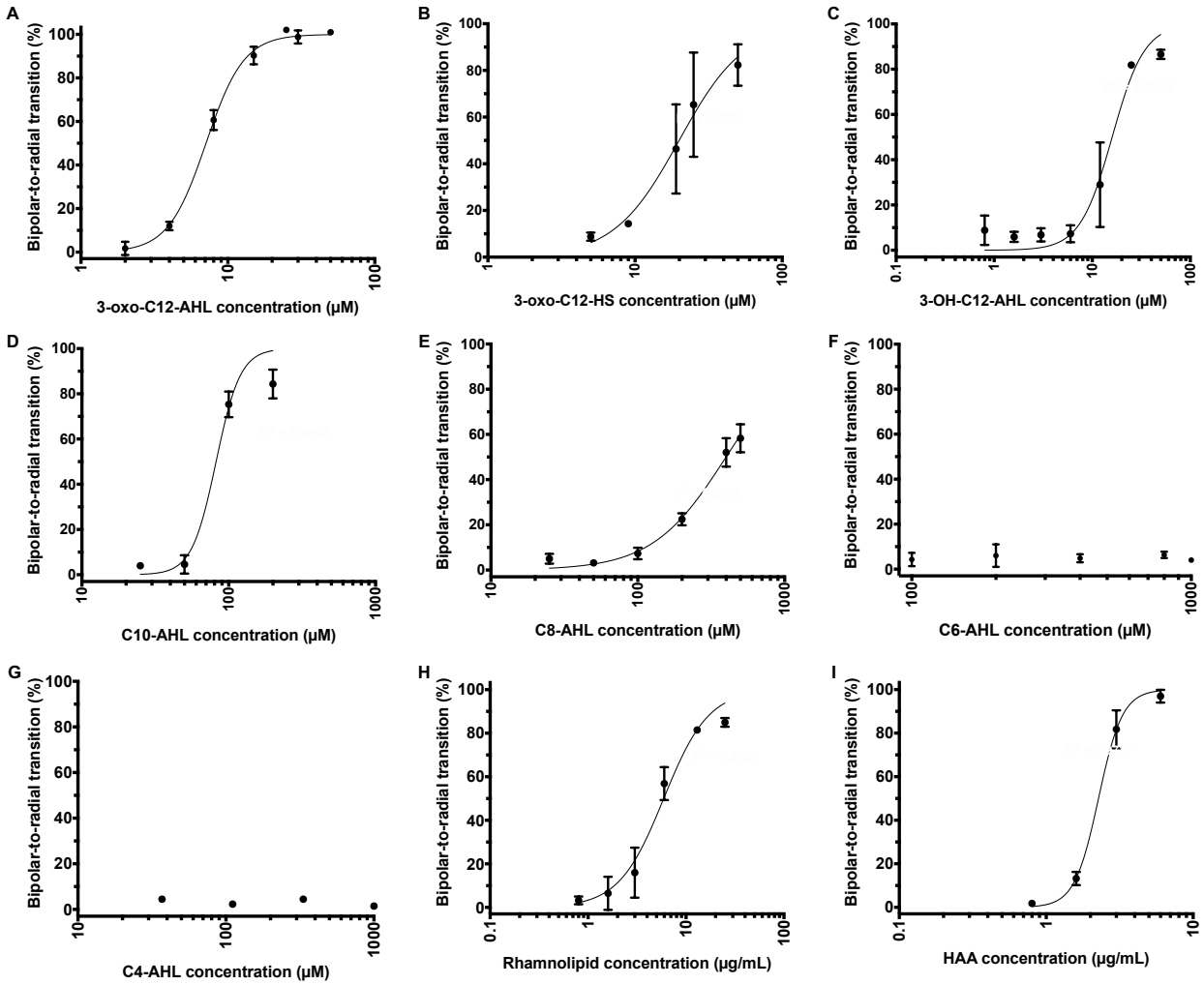

Figure S3. Plots of the percentage of LC droplets transformed from bipolar to radial as a function of the concentration of (A) 3-oxo-C12-AHL, (B) 3-oxo-C12-HS, (C) 3-OH-C12-AHL, (D) C10-AHL, (E) C8-AHL, (F) C6-AHL, (G) C4-AHL, (H) rhamnolipid, and (I) HAA in PBS with 10 μM SDS and 1% DMSO. Curves represent sigmoidal regressions used to obtain BR_{50} values using GraphPad Prism and a variable response sigmoidal model. Graphs were obtained from scattering plot analyses shown in Figure 3 of the main text and Figure S2 and are representative of three independent experiments with error bars representing the SEM.

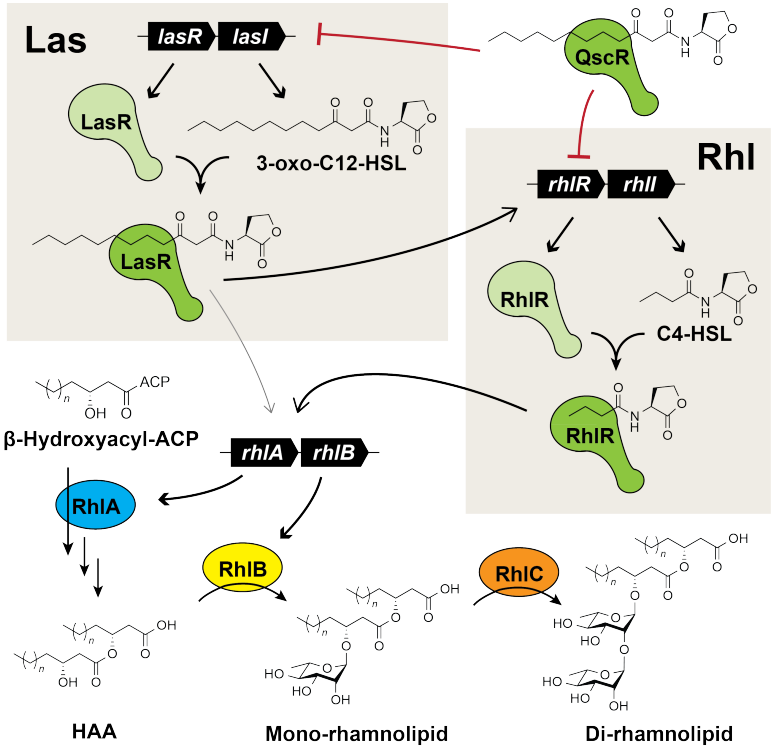

Figure S4. Detailed schematic of QS regulatory pathways used by *P. aeruginosa* to control rhamnolipid synthesis. QscR serves as a repressor for the Las and Rhl systems, and Las upregulates the Rhl system. Both LasR and RhlR upregulate the production of the rhlAB operon. RhlA helps to convert β-hydroxyacyl-acyl carrier proteins to 3-(3-hydroxyalkanoyloxy)alkanoic acids (HAAs). RhlB and RhlC sequentially add rhamnose sugars to HAAs. Solid arrowheads indicate positive regulation, while flat red arrowheads indicate negative regulation. Darker and lighter arrow colors indicate major and minor regulatory pathways, respectively.

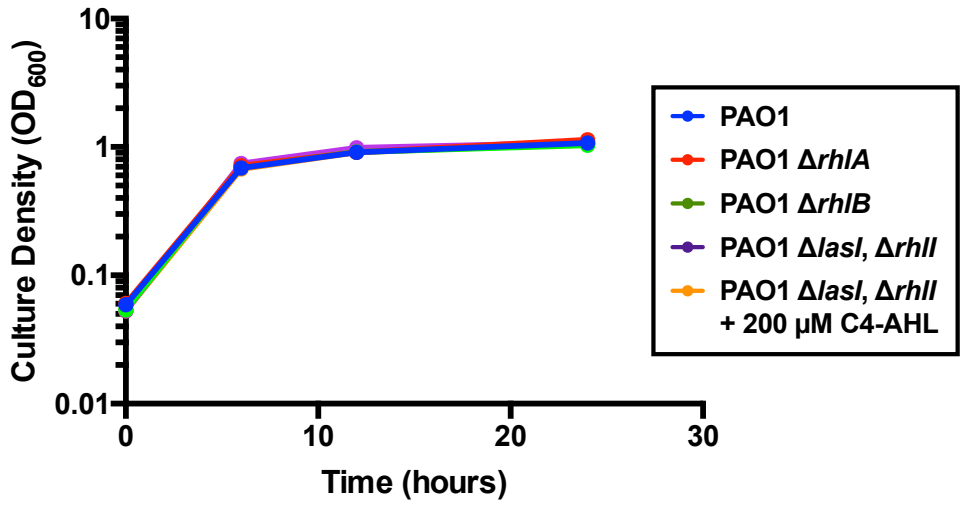

Figure S5. Optical density of bacterial cultures at 0, 6, 12, and 24 h determined by measuring absorbance at 600 nm. Comparable growth was observed for all strains. Results are the average of 3 independent experiments; error bars for SEM are too small to be shown.

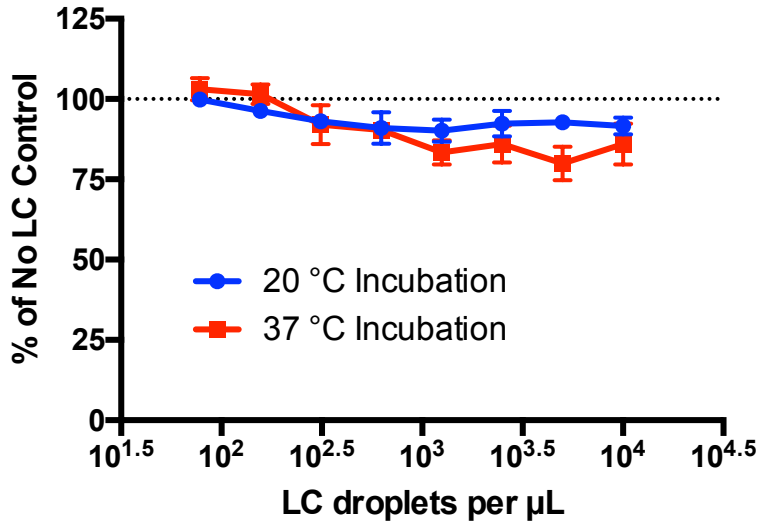

Figure S6. Plot of P. aeruginosa PAO1 viability upon incubation with varying concentrations of 5CB LC droplets vs. untreated (No LC) control. Cells were grown statically in 1:1 PBS:LB for 90 min. Results are the average of 3 independent experiments; error bars represent SEM.

Quantification of AHL and Rhamnolipid Concentrations in Bacterial Cultures

We performed analytical studies to estimate the concentrations of 3-oxo-C12-AHL and rhamnolipid produced by cultures of the *P. aeruginosa* strains used above and compare them to the values observed to promote bipolar-to-radial transformations in defined buffer (*e.g.,* Figure 3, Table 1 in the main text). For these experiments, aliquots of culture supernatant were removed at 6, 12, or 24 h, and the amounts of C4-AHL and 3-oxo-C12-AHL and their hydrolyzed ring-opened derivatives (C4-HS and 3-oxo-C12-HS) were quantified using a previously reported MS method developed in our laboratory (described above).[4] Results for 3-oxo-C12-AHL and 3-oxo-C12-HS are shown in Figures S7A and S8; results for C4-AHL and C4-HS are included in Figure S9. As anticipated, 3-oxo-C12-AHL was only observed to be present in cultures of the wild-type PAO1, PAO1 Δ*rhlB*, and PAO1 Δ*rhlA* strains, and these strains exhibited similar 3-

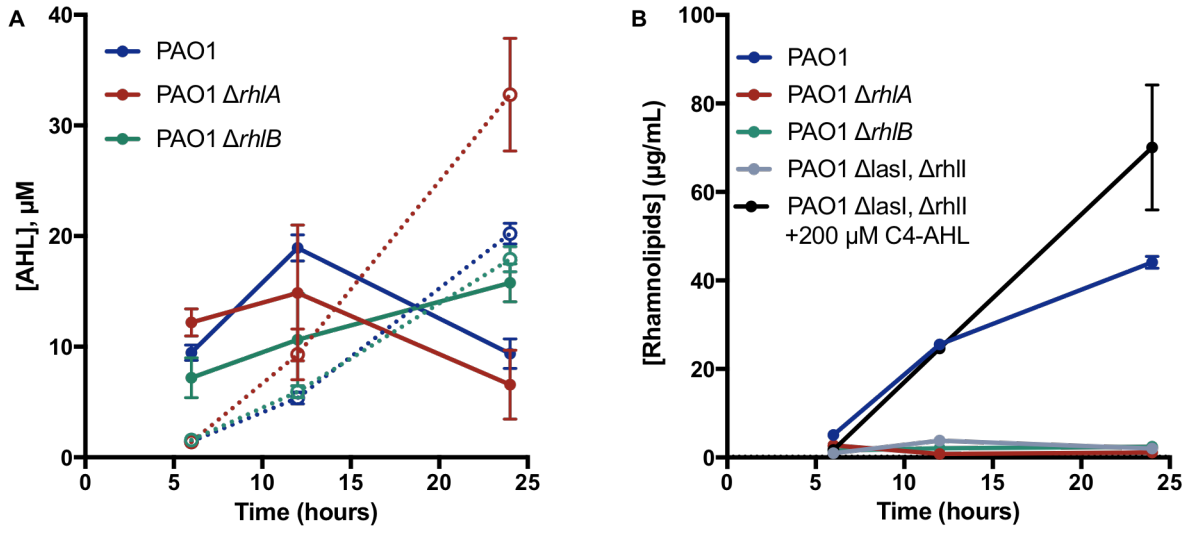

Figure S7. (A) Plot showing concentrations of 3-oxo-C12-AHL (solid lines) and 3-oxo-C12-HS (dotted lines) measured in the supernatants of wild type, Δ*rhlA*, and Δ*rhlB P. aeruginosa* cultures grown for 6, 12 and 24 h. Total hydrolyzed and unhydrolyzed 3-oxo-C12-AHL and C4-AHL concentrations are shown in Figures S8 and S9. (B) Plot showing concentrations of rhamnolipids measured in supernatants of wild type, Δ*rhlA*, and Δ*rhlB* cultures grown for 6, 12, and 24 h. Results are the average of 3 independent experiments; error bars represent SEM.

oxo-C12-AHL and 3-oxo-C12-HS concentration profiles over time. Inspection of Figure S7A (solid lines) reveals concentrations of 3-oxo-C12-AHL ranging from 7 to 12 μM after 6 h, followed by an increase to 12 to 19 μM after 12 h. Further inspection reveals 3-oxo-C12-AHL to decrease to 6 to 15 μM after 24 h. In contrast, concentrations of 3-oxo-C12-HS (dotted curves) increased, in a manner that was approximately linear, from 1 μM to ~20 to 30 μM over the same period. These differences are consistent with the gradual hydrolysis of 3-oxo-C12-AHL;[5] overall, these concentrations of 3-oxo-C12-AHL are consistent with levels reported in past studies on cultures of *P. aeruginosa.*[4,6]

We also estimated the concentration of rhamnolipid at each time point using an orcinol-based colorimetric assay that quantifies rhamnose sugars associated with rhamnolipid head groups.[7] Rhamnolipid was observed only in the wild-type PAO1 strain or in experiments in which exogenous C4-AHL was added to cultures of the PAO1 Δ*lasI*, Δ*rhlI* knockout strain to activate the RhlR system (Figure S7B). Concentrations of rhamnolipid increased monotonically over time for both strains, with amounts of rhamnolipid in cultures of PAO1 Δ*lasI*, Δ*rhlI* with added C4-AHL exceeding those measured in the wild-type strain by ~50% at 24 h. The concentrations observed in cultures of the wild-type strain are consistent with literature values.[8] While past studies have suggested that rhamnolipid levels cannot be fully recovered to wild-type levels without activation of the Las system,[9] these results suggest that increased production of rhamnolipid can occur at sufficiently high concentrations of C4-AHL.

The results in Figure S7 are consistent with the results shown in Figure 4 of the main text and provide additional support for the view that 3-oxo-C12-AHL, 3-oxo-C12-HS, and rhamnolipid produced in cultures of *P. aeruginosa* are responsible, either alone or in combination, for promoting transitions in LC droplets. We note that the levels of rhamnolipid

measured, under the culture conditions used here, for the wild-type strain at 12 and 24 h (~25 to 45 μg/mL) far exceed those observed to be necessary to promote radial transitions in >50% of the LC droplets in our experiments using defined buffer (6 μg/mL; Figure 3 and Table 1 of the main text). This observation is consistent with the robust responses in the LC droplets observed at these time points in our *in situ* experiments using this strain, shown in Figure 4 of the main text. The percentage of radial droplets was observed to be low at 6 h in those experiments, consistent with the fact that rhamnolipid is not produced in cultures of wild-type *P. aeruginosa* prior to reaching quorum.

Finally, we note that our results using LC droplets in defined buffer reveal 3-oxo-C12-AHL and 3-oxo-C12-HS to promote radial transitions in >50% of the droplets at concentrations of 7.1 μM and 20 μM, respectively. However, when LC droplets were incubated *in situ*, we observed cultures of the PAO1 Δ*rhlA* strain, which produces 3-oxo-C12-AHL and not rhamnolipid or HAA, to promote transitions in only ~15% of LC droplets incubated after 24 h (Figure 4 of the main text), even though the concentrations of 3-oxo-C12-AHL and 3-oxo-C12-HS were measured to be on the order of these threshold values at 12 and 24 h. The reasons for the reduced response of the LC droplets to 3-oxo-C12-AHL in this *in situ* environment are not currently understood; however, we note that these amphiphiles can adsorb onto surfaces and associate with or insert into components of cellular membranes, which could reduce effective concentrations.[10-12] It is also possible that competitive adsorption or partitioning of other species into the LC could lead to changes in elastic properties and thus changes in response. Our current results also do not permit conclusions regarding the effects that the adsorption of combinations of 3-oxo-C12-AHL and 3-oxo-C12-HS may have on the responses of the LC droplets. Nevertheless, our results make clear that, under the conditions used here, the majority of the

robust response in the LC droplets observed upon exposure to complex media containing growing bacterial cultures can be attributed to the presence of rhamnolipid and/or HAA that is produced once quorate populations are reached. In comparison to AHLs, the concentrations of these analytes measured in culture far exceed those of the BR_{50} values shown in Table 1.

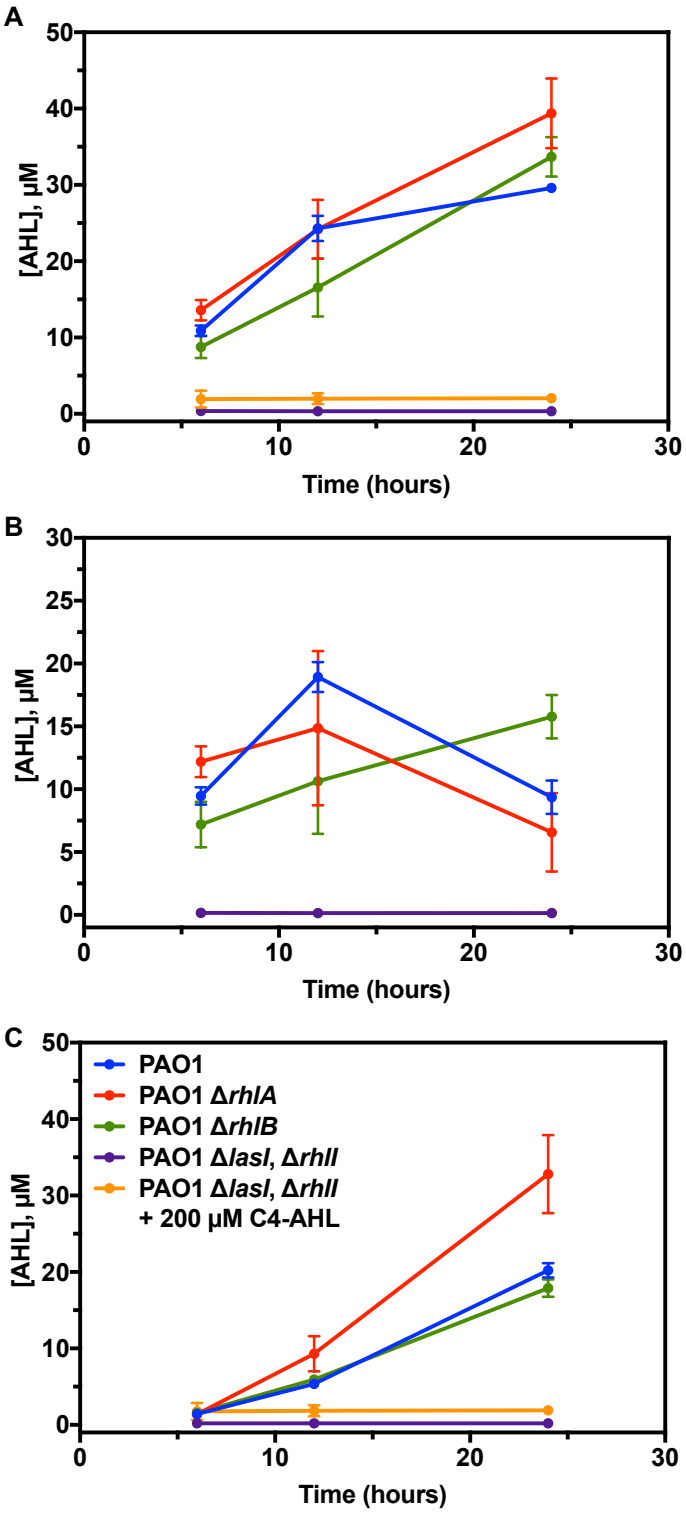

Figure S8. Concentrations of (A) total hydrolyzed and unhydrolyzed 3-oxo-C12-AHL, (B) unhydrolyzed 3-oxo-C12-AHL, and (C) 3-oxo-C12-HS in various *P. aeruginosa* strains grown for 6, 12 and 24 h as determined by HPLC-MS/MS analysis of 3 independent culture supernatants. Error bars represent the SEM.

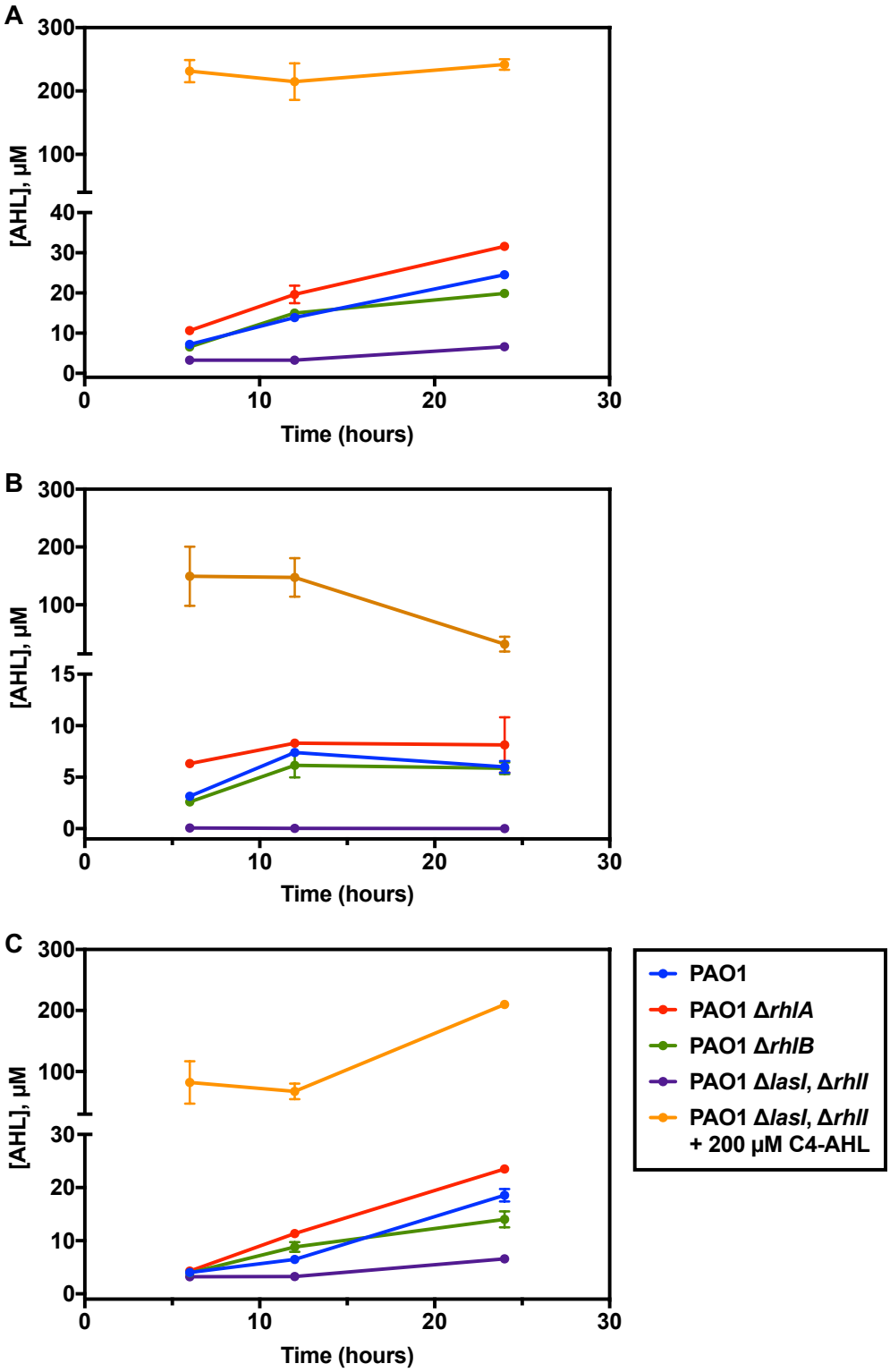

Figure S9. Concentrations of (A) total hydrolyzed and unhydrolyzed C4-AHL, (b) unhydrolyzed C4-AHL, and (C) C4-HS in various *P. aeruginosa* strains grown for 6, 12 and 24 h as determined by HPLC-MS/MS analysis of 3 independent culture supernatants. Error bars represent the SEM.

Supplementary Chemical Methods: Synthesis and Characterization of 3-(3-Hydroxyalkanoyloxy)-alkanoic acid) (HAA)

The synthesis of racemic HAA was adapted from reported procedures [Carrocci, Tucker Joe. Synthesis and Characterization of 3-(3-Hydroxyalkanoyloxy)alkanoic acids (HAAs). Bachelor's Honors Thesis. University of Arizona, Tucson, AZ, 2011.], and is outlined in Scheme S1 below.

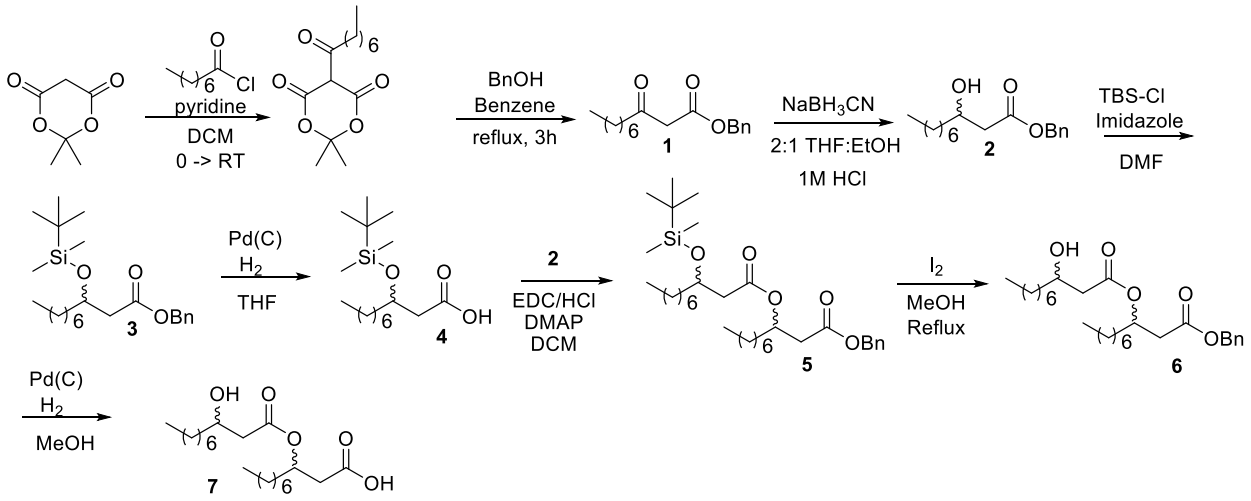

Scheme S1. Synthesis of racemic 3-(3-hydroxyalkanoyloxy)alkanoic acid (HAA, **7**).

Materials and Methods

Reagents and solvents were purchased commercial sources (Sigma-Aldrich, TCI America, or Acros Organics) and used without further purification, except for ethyl acetate, hexanes, and dichloromethane, which were distilled before use, and Meldrum's acid, which was recrystallized from tert-butyl methyl ether. Thin layer chromatography (TLC) was performed on 250 μm silica plates from Silicycle with F_{254} UV indicator. Plates were visualized with UV light or bromocresol green stain. Silica Gel 60 (230-400 mesh) from Macherey-Nagel was used for flash column chromatography. All proton and carbon NMR spectra were recorded on a Bruker

Avance-400 MHz spectrometer. Chemical shifts are reported in ppm relative to solvent peaks as internal standards set to δ 7.26 and δ 77.16 ($CDCl_3$). NMR data are reported as: chemical shift, multiplicity (s = singlet, bs = broad singlet d = doublet, dd = doublet of doublets, t = triplet, p = pentet, m = multiplet, ABX = ABX system), coupling constant (Hz), and integration. High-resolution mass spectra (HRMS) were recorded on a Q Extractive Plus Orbitrap with an electrospray ion source.

*Synthesis of benzyl-3-oxodecanoate (**1**)*

To a flame dried 100 mL round bottom flask (RBF) charged with dichloromethane (DCM, 25 mL) was added Meldrum's acid (10g, 69 mmol) and pyridine (13.6 mL, 170 mmol). The solution was cooled to 0 °C and octanoyl chloride (10.75 mL, 63 mmol), dissolved in DCM (25 mL), was added. The reaction was stirred for 1 h at 0 °C, then warmed to room temperature and stirred for an additional two hours. The reaction mixture was then partitioned with 1M HCl. The organic layer was washed with 1M HCl (3 x 100 mL) and water (1 x 100 mL). The organic portion was dried over $MgSO_4$ and concentrated under reduced pressure to yield a red oil (15.5 g). That oil was dissolved in benzene (70 mL). Benzyl alcohol (17.9 mL, 172 mmol) was added and the reaction was refluxed for four hours. Concentration under reduced pressure and flash chromatography (20% EtOAc/Hex) yielded the desired product (**1**) as a yellow oil (15.9 g isolated, 83% isolated yield over 2 steps). ^{1}H NMR (400 MHz, $CDCl_3$) δ 7.31-7.39 (m, 5H), 5.16-5.18 (s, 2H), 3.47-3.49 (s, 2H) 2.47-2.52 (t, 2H, J = 7 Hz) 1.52-1.6 (p, 2H, J = 7 Hz), 1.20-1.34 (m, 8H), 0.86-0.90 (t, J = 7 Hz, 3H).

*Synthesis of benzyl-3-hydroxydecanoate (**2**)*

Compound **1** (4.5 g, 16 mmol) was dissolved in a 2:1 mixture of tetrahydrofuran (THF): ethyl alcohol (25 mL : 12.5 mL) and stirred at 0 °C. Sodium borohydride (2.12g, 32 mmol) was added and the reaction was allowed to warm to room temperature as aqueous 1M HCl (32 mL) was added via an addition funnel. After addition was complete, the reaction was extracted with DCM (3 x 75 mL). The combined organic portion was dried over MgSO4 and concentrated under reduced pressure. The product (**2**) was used without further purification (97% crude yield). ^{1}H NMR (400 MHz, $CDCl_3$) δ 7.31-7.40 (m, 5H), 5.15-5.17 (s, 2H), 3.98-4.06 (m, 1H), 2.81-2.96 (bs, 1H), 2.43-2.59 (AB of ABX, J_{AB} = 16 Hz , J_{AX} = 3Hz , J_{BX} = 8.97 Hz), 1.36-1.47 (m, 2H) 1.21-1.37 (m, 10H), 0.84-0.91 (t, J = 7H, 3H).

*Synthesis of benzyl-3-((tert-butyldimethylsislyl)oxy)decanoate (**3**)*

To a solution of compound **2** (4.3g, 15.4 mmol) in dimethylformamide (DMF, 15 mL) was added *tert*-butyldimethylsilyl chloride (TBS-Cl, 2.8g, 18.5 mmol) and imidazole (2.1g, 30.9 mmol). The reaction was allowed to stir overnight. The reaction was diluted with water (125 mL) and extracted with diethyl ether (3 x 100 mL). The organic portion was washed with brine (3 x 25 mL), dried over $MgSO_4$ and concentrated under reduced pressure. Flash chromatography (5-10% EtOAc/Hex gradient) gave the desired product (**3**; 4.13 g, 68% isolated yield). ^{1}H NMR (400 MHz, $CDCl_3$) δ 7.24-7.34 (m, 5H), 5.02-5.09 (AB quartet, Jab = 12 Hz), 4.05-4.12 (m, 1H), 2.38-2.48 (AB of ABX, J_{AX} = 7 Hz , J_{BX} = 6 Hz, J_{AB} = 15 Hz, 2H), 1.38-1.45 (m, 2H), 1.15-1.29 (m ,10H) 0.78-0.85 (m, 12H), -0.01 - 0.01 (s = 3H), -0.04 - -0.02 (s, 3H).

*Synthesis of 3-((tert-butyldimethylsilyl)oxy)decanoic acid (**4**)*

To a flame-dried RBF was added Pd/C (10% wt, 1.17g, 1.05 mmol). The atmosphere was exchanged for nitrogen. Dry THF was added until a slurry formed. Compound **3** (4.13 g, 10.5 mmol) was dissolved in dry THF (105 mL) and added. The atmosphere was exchanged for hydrogen, and the reaction was allowed to proceed overnight. The reaction mixture was poured over a celite plug, and compound was eluted with DCM. Flash chromatography (25% EtOAc/hex) yielded the desired product as a mixture of diastereomers (437 mg, 14% isolated yield). ^{1}H NMR (400 MHz, $CDCl_3$) δ 4.04-4.12 (apparent p, J = 6 Hz, 1H) 2.45-2.59 (m, 2H) 1.47-1.59 (m, 1H), 1.21-1.34 (m, 10H) 0.84-0.93 (s, 9H overlapping with t, J = 7H, 3H), 0.08-0.11 (two overlapping s, 6H).

*Synthesis of benzyl 3-((3-((tert-butyldimethylsilyl)oxy)decanoyl)oxy)decanoate (**5**)*

Acid **4** (100 mg, 0.33 mmol) was dissolved in dry DCM (1mL). Alcohol **3** (97 mg, 0.348 mmol) was dissolved in dry DCM (1.5 mL) and added to the reaction mixture. 4-(Dimethylamino)pyridine (DMAP; 20 mg, 1.7 mmol) and (3-dimethylaminopropyl)-*N*'-ethylcarbodiimide hydrochloride (EDC/HCl; 190 mg, 0.49 mmol) were added sequentially. The reaction was stirred for 24 h at room temperature. The reaction was then diluted in 10 mL H_2O and extracted with DCM (3 x 10 mL). The organic portion was washed with 1M HCl (2 x 15 mL) and brine (1 x 15 mL), then dried over $MgSO_4$ and concentrated under reduced pressure. Flash chromatography (0-5% EtOAc/Hex gradient) yielded the desired product (**5**) as a mixture of diastereomers (172 mg, 69% isolated yield). ^{1}H NMR (400 MHz, $CDCl_3$) δ 7.29-7.39 (m, 5H), 5.17-5.26 (m, 1H), 5.10-5.12 (apparent d, J = 2Hz, 2H), 4.03-4.11 (m, 1H), 2.53-2.26 (m, 2H),

2.23-2.43 (m, 2H) 1.54-1.64 (m, 2H), 1.40-1.48 (m, 2H), 1.21-1.34 (m, 20H) 0.85-0.9 (m, 15H), 0.03-0.06 (m, 6H).

*Synthesis of benzyl 3-((3-hydroxydecanoyl)oxy)decanoate (**6**)*

Compound **5** (128 mg, .23 mmol) was dissolved in a 1% m/v solution of I_2 in methanol (13 mL). The reaction was heated to reflux until TLC indicated consumption of starting material (6.5 h). The reaction was quenched by addition of aqueous 10% sodium thiosulfate (8 mL). Flash chromatography (5-25% EtOAc/Hex gradient) yielded the desired product (**6**) as a mixture of diastereomers (68 mg, 67% isolated yield). ^{1}H NMR (400 MHz, $CDCl_3$) δ 7.29-7.39 (m, 5H) 5.2-5.32 (m, 1H), 5.11-5.12 (s, 2H), 3.88-4.0 (m, 1H), 2.93-3.07 (dd, J = 30 Hz, 4Hz, 1H), 2.57-2.66 (m, 2H), 2.28-2.45 (m, 2H) 1.20-1.66 (m, 24H), 0.84-0.91 (m, 6H).

*Synthesis of 3-((3-hydroxydecanoyl)oxy)decanoic acid (HAA, **7**)*

To a flame dried RBF was added Pd/C (10% 12 mg, 0.01 mmol) and the atmosphere was exchanged for nitrogen. Sufficient DCM was added to form a slurry. Compound **6** (51 mg, 0.11 mmol) was dissolved in MeOH (1.1 mL) and added to the reaction vessel. The atmosphere was exchanged for hydrogen, and the reaction was allowed to proceed overnight. The next day, the atmosphere was exchanged for nitrogen, and the reaction mixture was filtered over celite. The reaction mixture was concentrated under reduced pressure. Flash chromatography (5% MeOH, 95% DCM) afforded the desired product (HAA, **7**) as a mixture of diastereomers (12 mg, 24% isolated yield). ^{1}H NMR (400 MHz, $CDCl_3$) δ 5.22-5.29 (m, 1H), 3.98-4.05 (m, 1H), 2.31-2.65 (m, 4H) 1.16-1.7 (m, 24H), 0.85-0.91 (t, J = 7 Hz); ^{13}C NMR (400 MHz, $CDCl_3$) δ 175.10, 172.16, 70.76, 68.36, 41.97, 38.74, 36.55, 34.13, 31.95, 31.88, 29.85, 29.65, 29.41, 29.38, 29.26,

25.29, 22.80, 22.76, 14.25, 14.22; HRMS $[M-H]^-$ calculated m/z = 357.2647, observed m/z = 357.2648.

NMR spectra for synthetic intermediates 1–6 and HAA (7)

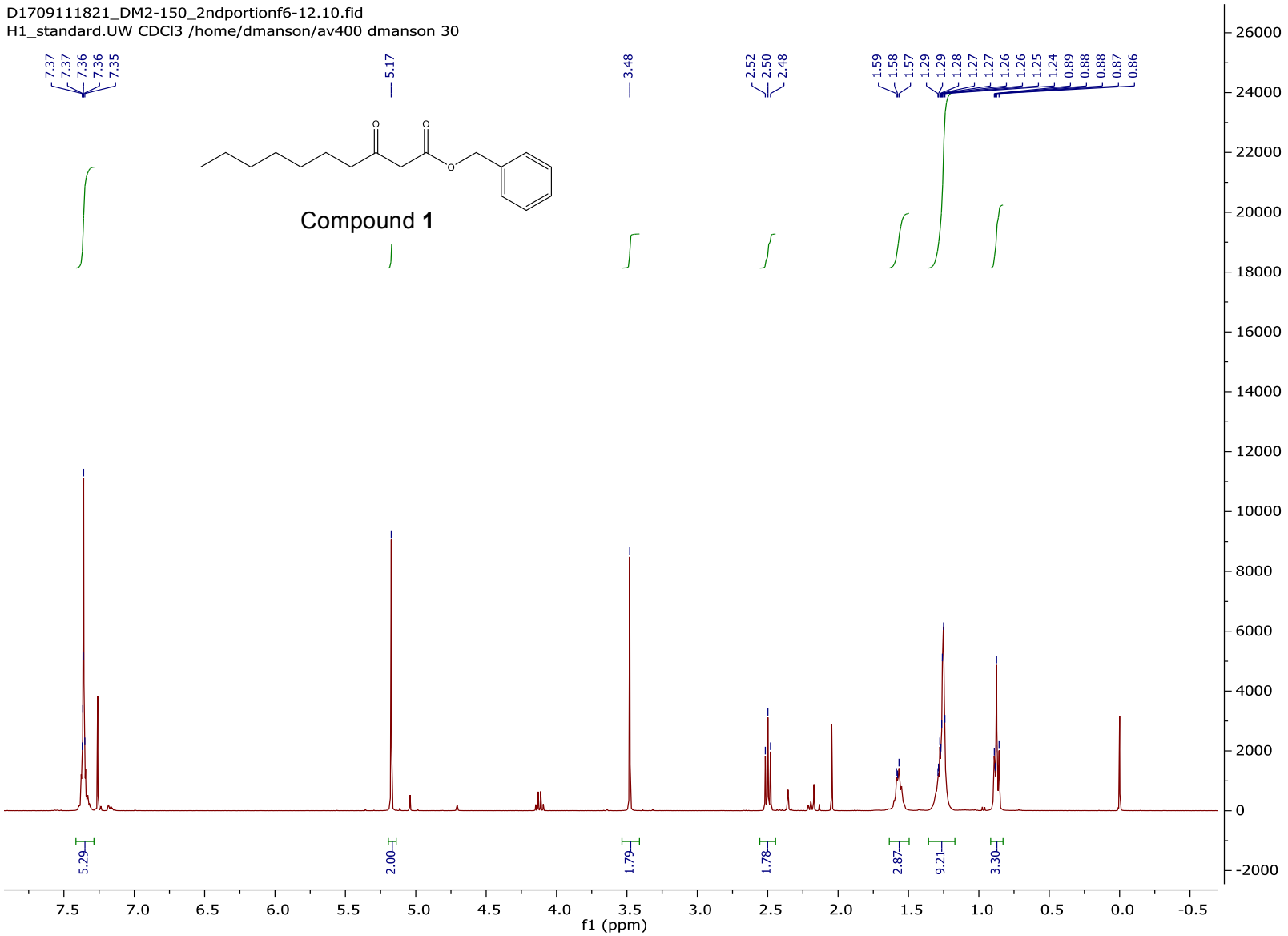

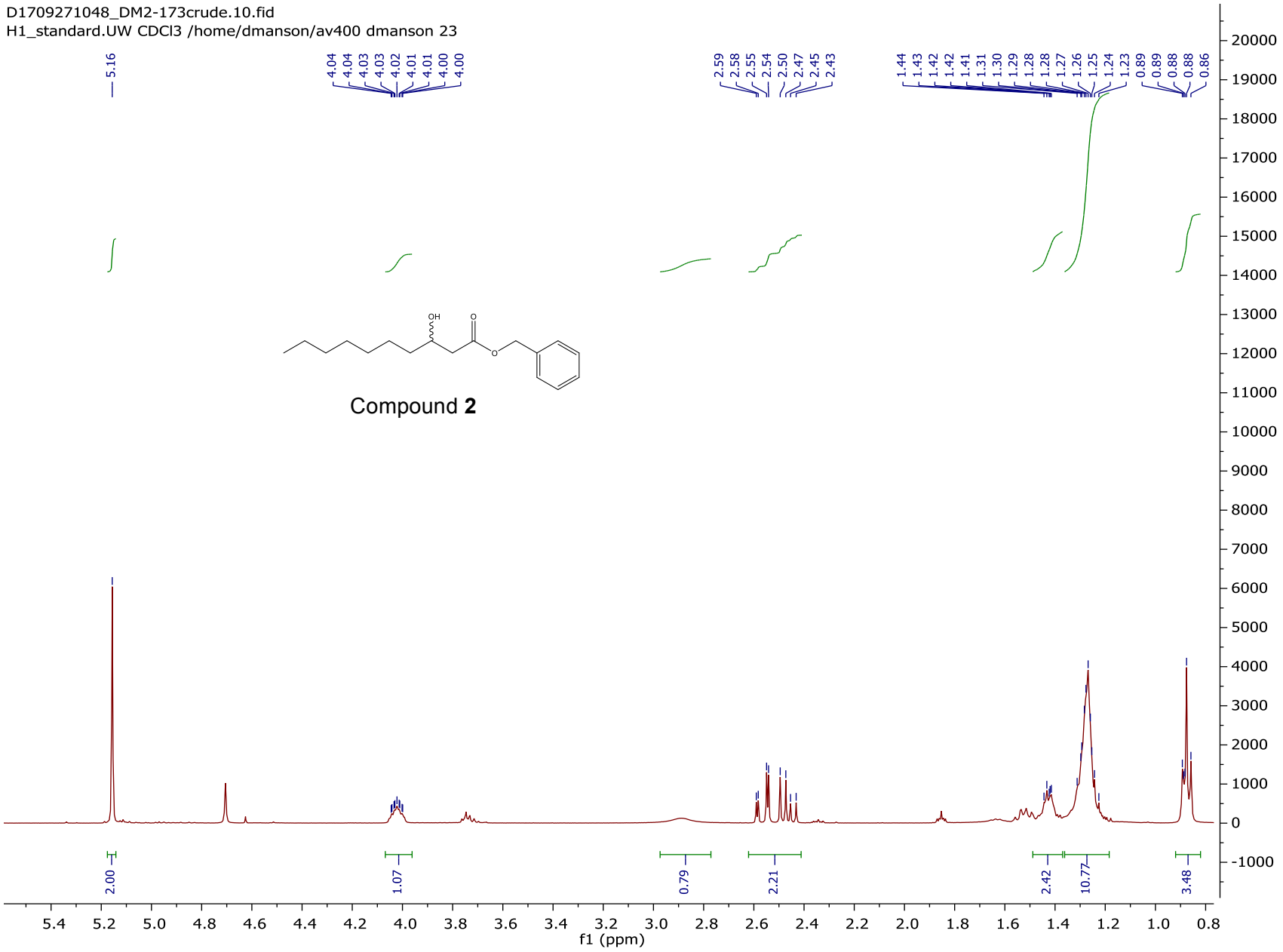
D1709271048_DM2-173crude.10.fid
H1_standard.UW CDCl3 /home/dmanson/av400 dmanson 23
5.16
4.04 4.04 4.03 4.03 4.02 4.01 4.01 4.00 4.00
2.59 2.58 2.55 2.54 2.50 2.47 2.45 2.43
1.44 1.43 1.42 1.42 1.41 1.31 1.30 1.29 1.28 1.28 1.27 1.26 1.25 1.24 1.23
0.89 0.89 0.88 0.88 0.86
OH
O
O
Compound 2
2.00
1.07
0.79
2.21
2.42
10.77
3.48
f1 (ppm)

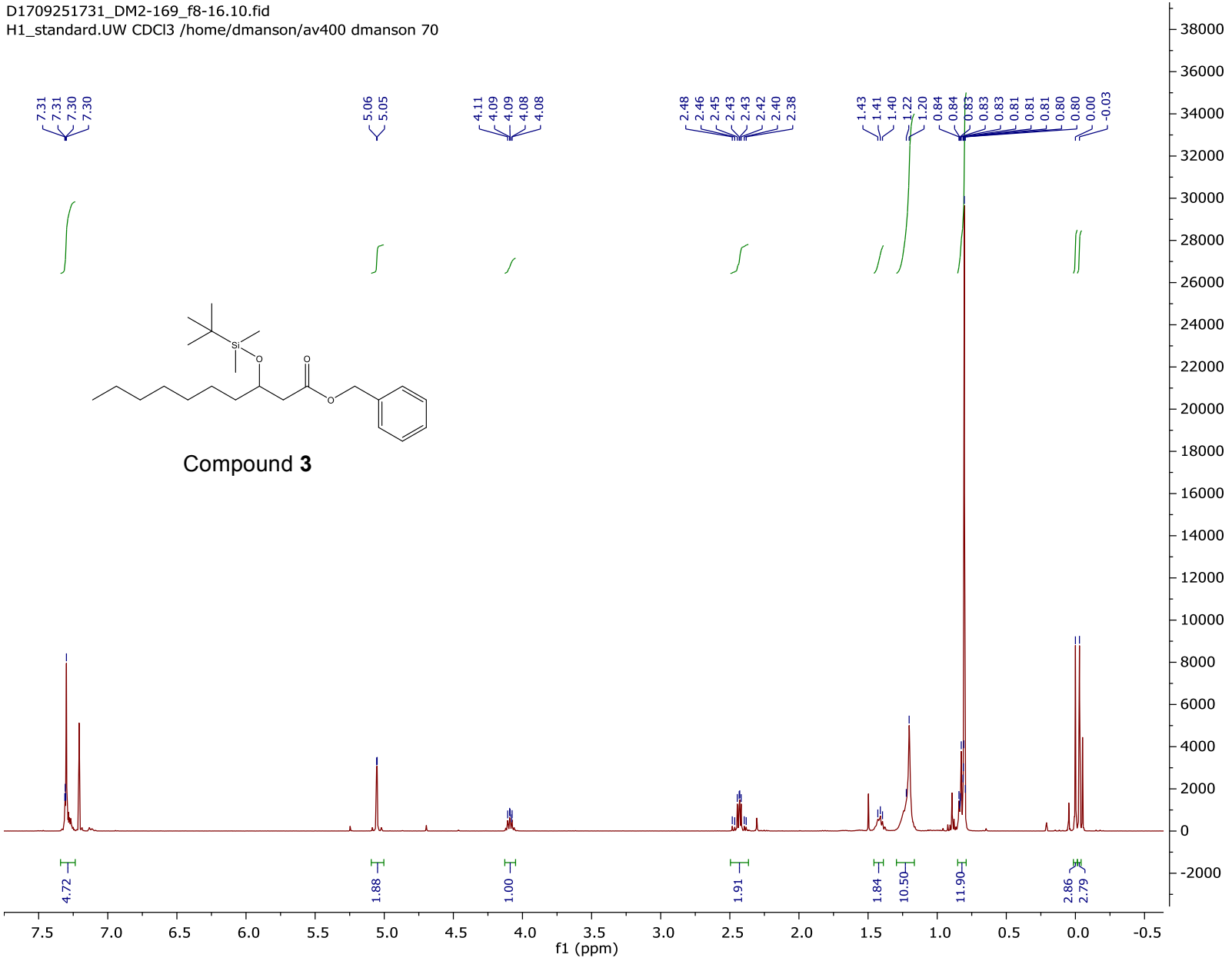
D1709251731_DM2-169_f8-16.10.fid
H1_standard.UW CDCl3 /home/dmanson/av400 dmanson 70
7.31
7.31
7.30
7.30
5.06
5.05
4.11
4.09
4.09
4.08
4.08
2.48
2.46
2.45
2.43
2.43
2.42
2.40
2.38
1.43
1.41
1.40
1.22
1.20
0.84
0.84
0.83
0.83
0.83
0.81
0.81
0.81
0.80
0.80
0.00
-0.03
Si
O
O
O
Compound 3
4.72
1.88
1.00
1.91
1.84
10.50
11.90
2.86
2.79
f1 (ppm)

D1801181752_DM2-172_f5-7.10.fid
H1_standard.UW CDCl3 /home/dmanson/av400 dmanson 17

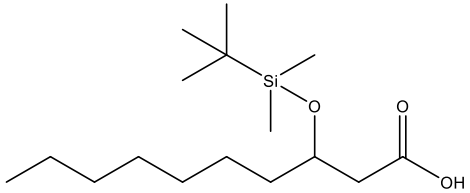

Compound **4**

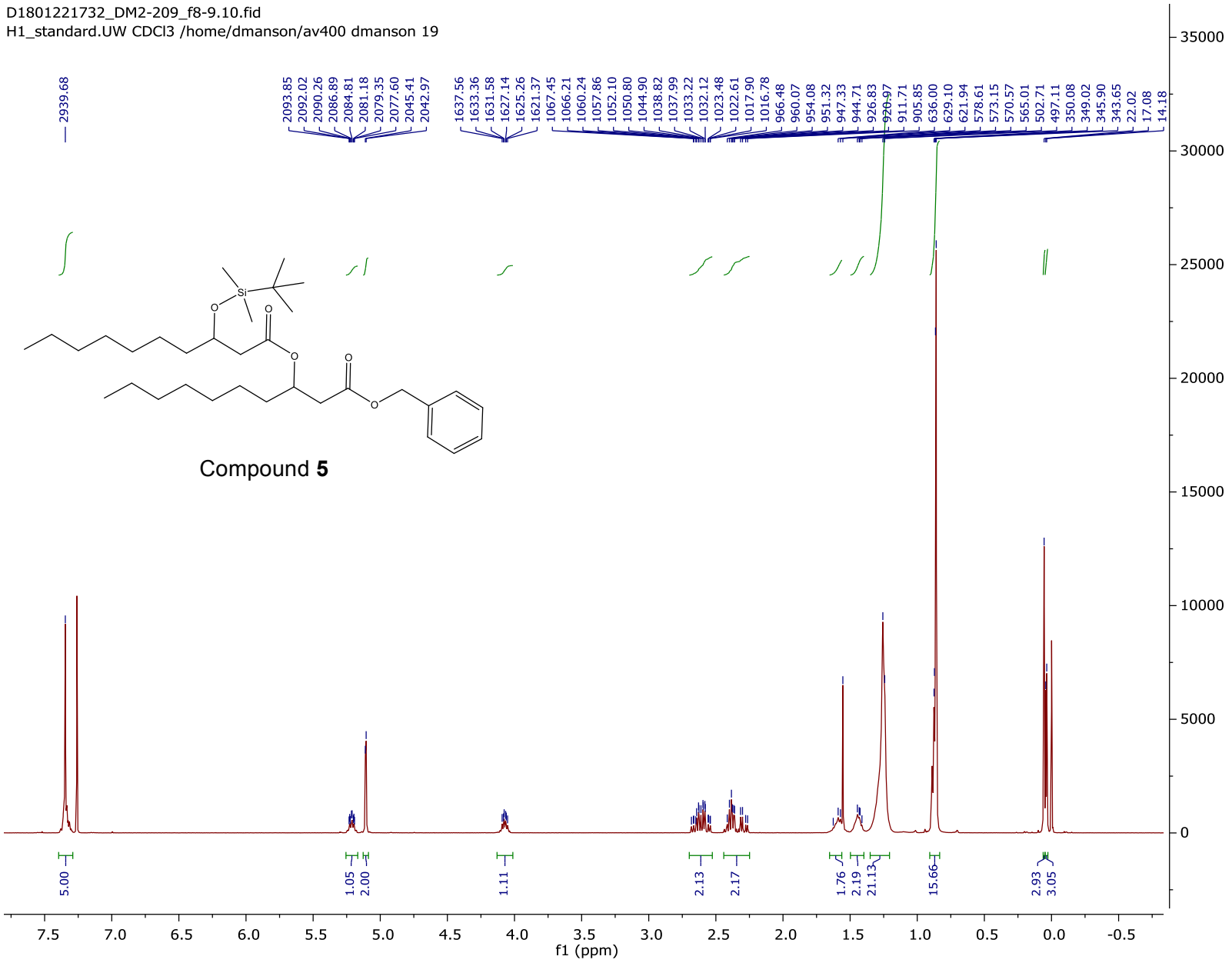
D1801221732_DM2-209_f8-9.10.fid
H1_standard.UW CDCl3 /home/dmanson/av400 dmanson 19
Compound 5
f1 (ppm)

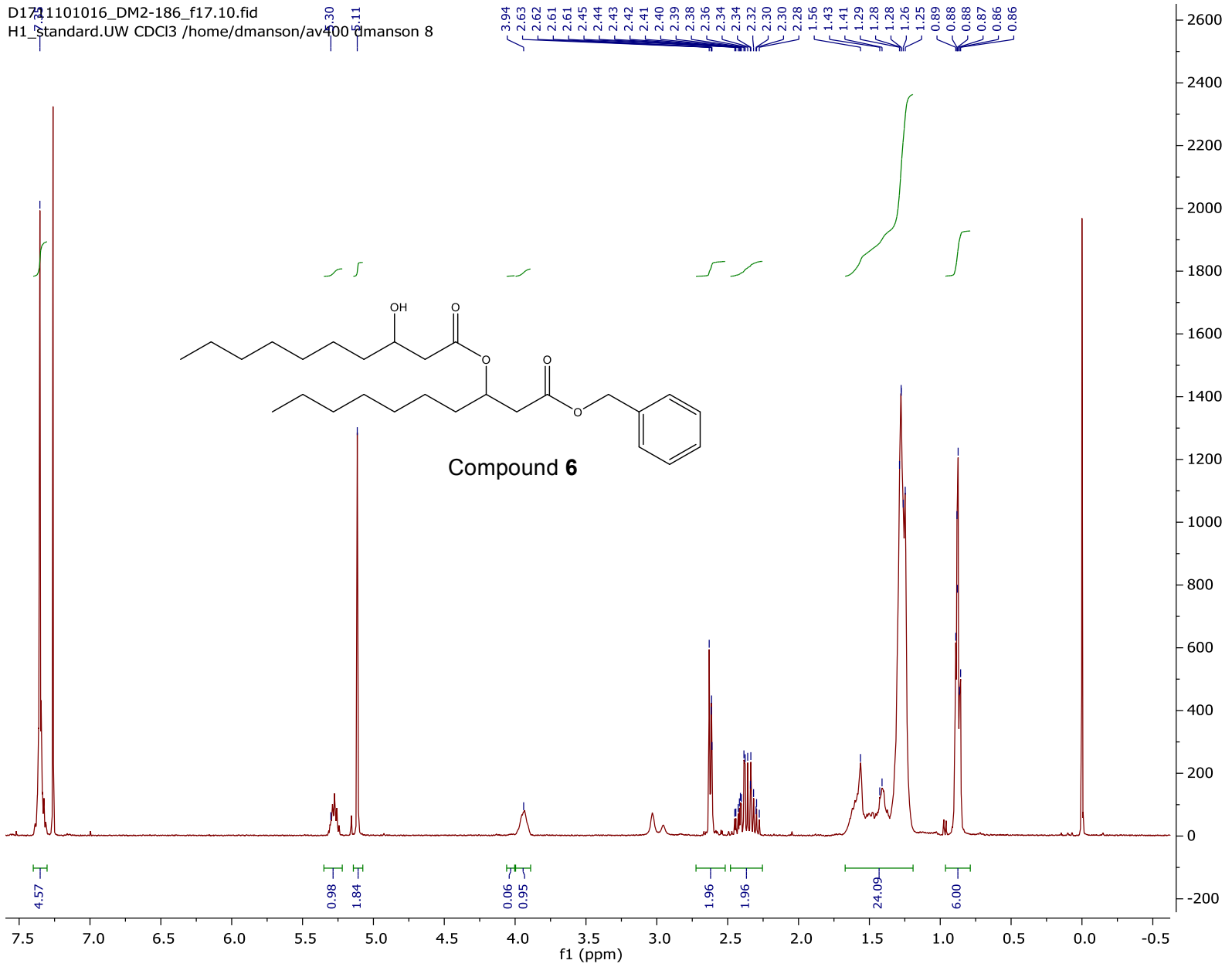
D17-1101016_DM2-186_f17.10.fid
H1_standard.UW CDCl3 /home/dmanson/av400 dmanson 8
7.30
5.11
3.94
2.63
2.62
2.61
2.61
2.45
2.44
2.43
2.42
2.41
2.40
2.39
2.38
2.36
2.34
2.34
2.32
2.30
2.30
2.28
1.56
1.43
1.41
1.29
1.28
1.28
1.26
1.25
0.89
0.88
0.88
0.87
0.86
0.86
OH
O
O
O
O
Compound 6
4.57
0.98
1.84
0.06
0.95
1.96
1.96
24.09
6.00
f1 (ppm)

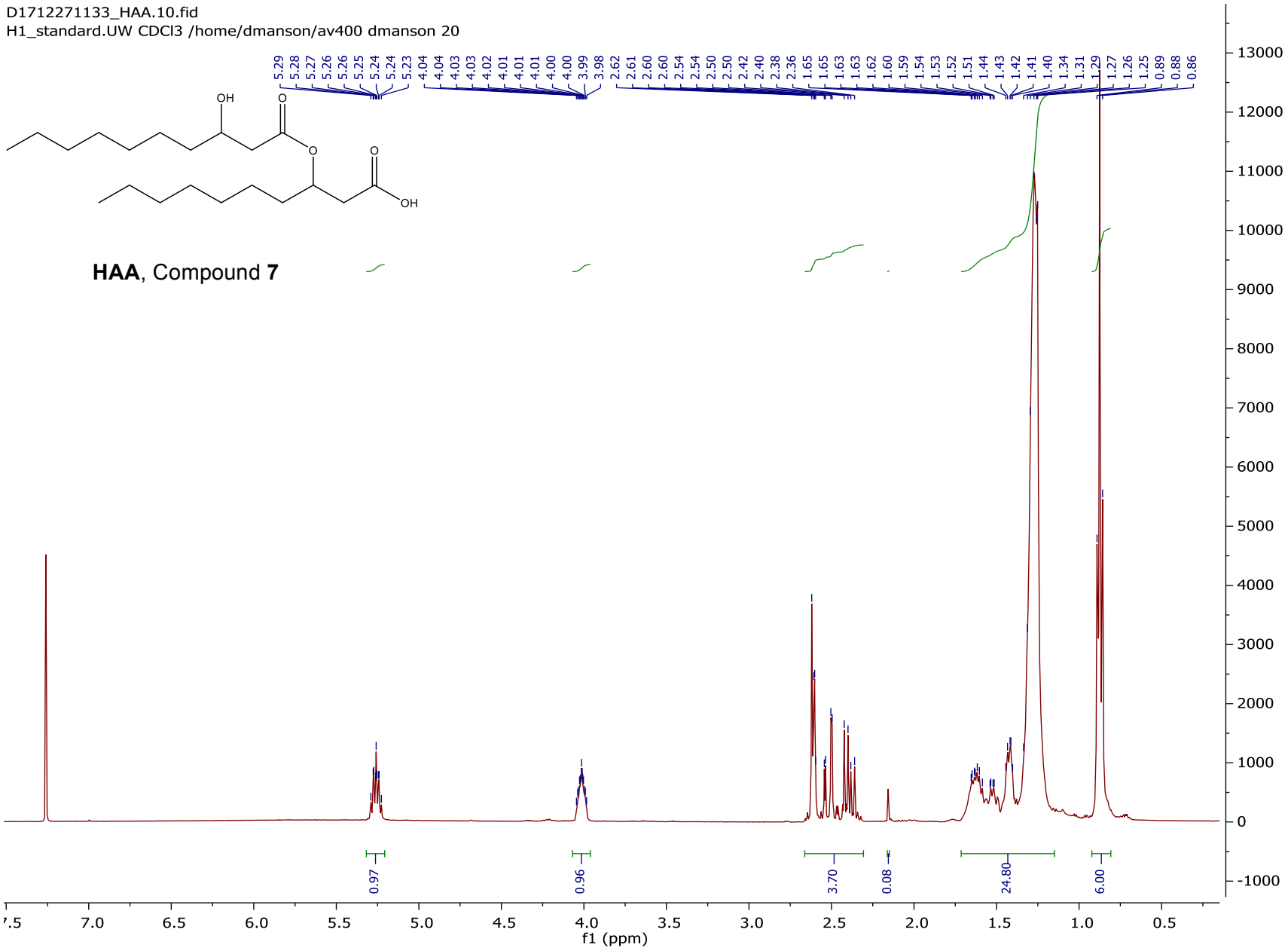
D1712271133_HAA.10.fid
H1_standard.UW CDCl3 /home/dmanson/av400 dmanson 20
OH
O
O
O
OH
HAA, Compound 7
f1 (ppm)

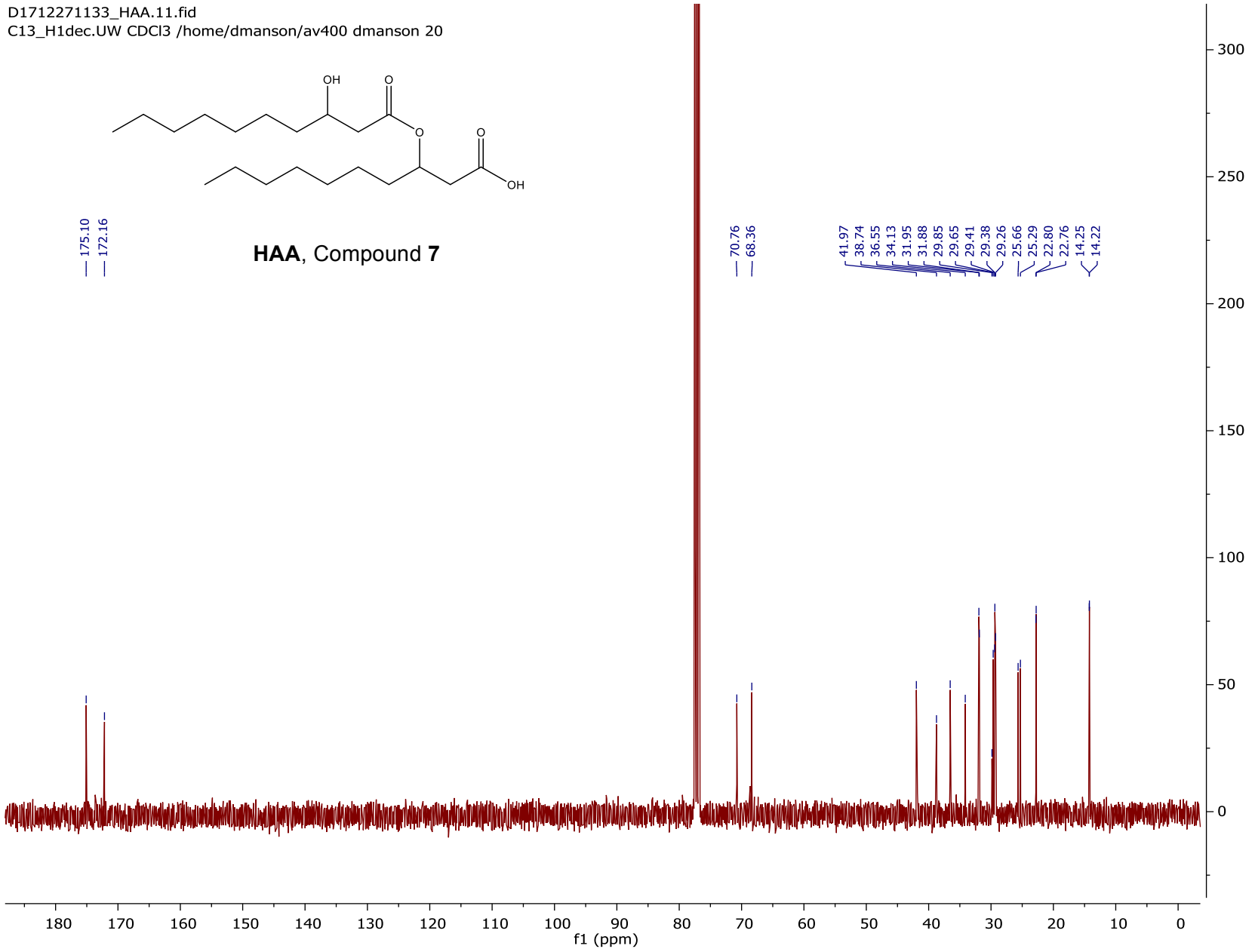
D1712271133_HAA.11.fid
C13_H1dec.UW CDCl3 /home/dmanson/av400 dmanson 20
OH
O
O
O
OH
HAA, Compound 7
175.10
172.16
70.76
68.36
41.97
38.74
36.55
34.13
31.95
31.88
29.85
29.65
29.41
29.38
29.26
25.66
25.29
22.80
22.76
14.25
14.22
300
250
200
150
100
50
0
180
170
160
150
140
130
120
110
100
90
80
70
60
50
40
30
20
10
0
f1 (ppm)

References

1. Holloway, B. Genetic recombination in pseudomonas aeruginosa. *Microbiology* **1955,** *13*, 572-581.

2. Jacobs, M. A.; Alwood, A.; Thaipisuttikul, I.; Spencer, D.; Haugen, E.; Ernst, S.; Will, O.; Kaul, R.; Raymond, C.; Levy, R. Comprehensive transposon mutant library of *pseudomonas aeruginosa*. *Proc. Natl. Acad. Sci. U. S. A.* **2003,** *100*, 14339-14344.

3. Smalley, N. E.; An, D.; Parsek, M. R.; Chandler, J. R.; Dandekar, A. A. Quorum sensing protects *pseudomonas aeruginosa* against cheating by other species in a laboratory coculture model. *J. Bacteriol.* **2015,** *197*, 3154-3159.

4. Patel, N. M.; Moore, J. D.; Blackwell, H. E.; Amador-Noguez, D. Identification of unanticipated and novel n-acyl l-homoserine lactones (ahls) using a sensitive non-targeted lc-ms/ms method. *PloS one* **2016,** *11*, e0163469.

5. Yates, E. A.; Philipp, B.; Buckley, C.; Atkinson, S.; Chhabra, S. R.; Sockett, R. E.; Goldner, M.; Dessaux, Y.; Cámara, M.; Smith, H. N-acylhomoserine lactones undergo lactonolysis in a ph-, temperature-, and acyl chain length-dependent manner during growth of yersinia pseudotuberculosis and pseudomonas aeruginosa. *Infection and immunity* **2002,** *70*, 5635-5646.

6. Davenport, P. W.; Griffin, J. L.; Welch, M. Quorum sensing is accompanied by global metabolic changes in the opportunistic human pathogen pseudomonas aeruginosa. *Journal of bacteriology* **2015,** *197*, 2072-2082.

7. Welsh, M. A.; Eibergen, N. R.; Moore, J. D.; Blackwell, H. E. Small molecule disruption of quorum sensing cross-regulation in pseudomonas aeruginosa causes major and unexpected alterations to virulence phenotypes. *Journal of the American Chemical Society* **2015,** *137*, 1510-1519.

8. Deziel, E.; Lepine, F.; Milot, S.; Villemur, R. Rhla is required for the production of a novel biosurfactant promoting swarming motility in *pseudomonas aeruginosa*: 3-(3-hydroxyalkanoyloxy) alkanoic acids (haas), the precursors of rhamnolipids. *Microbiology* **2003,** *149*, 2005-2013.

9. Pearson, J. P.; Pesci, E. C.; Iglewski, B. H. Roles of *pseudomonas aeruginosa* las and rhl quorum-sensing systems in control of elastase and rhamnolipid biosynthesis genes. *J. Bacteriol.* **1997,** *179*, 5756-5767.

10. Barth, C.; Jakubczyk, D.; Kubas, A.; Anastassacos, F.; Brenner-Weiss, G.; Fink, K.; Schepers, U.; Bräse, S.; Koelsch, P. Interkingdom signaling: Integration, conformation, and orientation of n-acyl-l-homoserine lactones in supported lipid bilayers. *Langmuir* **2012,** *28*, 8456-8462.

11. Toyofuku, M.; Morinaga, K.; Hashimoto, Y.; Uhl, J.; Shimamura, H.; Inaba, H.; Schmitt-Kopplin, P.; Eberl, L.; Nomura, N. Membrane vesicle-mediated bacterial communication. *The ISME journal* **2017,** *11*, 1504.

12. Davis, B. M.; Jensen, R.; Williams, P.; O'Shea, P. The interaction of n-acylhomoserine lactone quorum sensing signaling molecules with biological membranes: Implications for inter-kingdom signaling. *PloS one* **2010,** *5*, e13522.